

TRIUMF	UNIVERSITY OF ALBERTA EDMONTON, ALBERTA	
	Date 1996-07-30	File No. TRI-DNA-96-5
Author GM Stinson		Page 1 of 29
Subject A 480 MeV to 500 MeV beam transport system to an ISAC Facility		

1. Introduction

Recent reports^{1,2)} gave a detailed optical design for a beam line for the delivery of beam to an external ISAC. Since these reports were issued a revision of the complete facility has been undertaken. The major change is the rotation of the production targets such that the building in which they are located is perpendicular to the extraction beam line rather than parallel to it as in the initial layout. Further, only two target facilities are contemplated.

This report presents a final design for such a configuration.

2. Design Modifications

2.1 An overview

Figure 1, taken from ref¹⁾, shows the beam line configuration that was considered in the first proposal for an ISAC facility. Figure 2 presents the layout now considered to be the final version of the beam line. In each of these figures, and throughout this report, element locations are specified in a Cartesian coordinate system that is located with its origin $(x_0, y_0) = (0, 0)$ at the cyclotron center. The positive x -axis is directed east and the positive y -axis is directed north.

A major difference between the two proposals is that the configuration of figure 1 was designed to be achromatic throughout the beam line and slightly dispersed at the target locations, whereas that of figure 2 is designed to be dispersed throughout the beam line and spatially achromatic at the target locations.

It will be noted that three target locations are shown in figure 1. The intent of this was to allow for the possibility of the extraction of a split, or double, beam as proposed in ref³⁾ for use on beam line 1A. In this manner, it would be possible to feed two of the targets simultaneously—albeit neither target would receive full beam intensity. It should also be noted that this split beam proposal was just that; no study had been put into the optical requirements for such a beam line.

In contrast, figure 2 shows only two target locations. Beam would be switched between these two positions so that one target would be operational while the other was being repaired or its target material was being changed.

Extraction parameters for beam line 2A were calculated by R. Lee⁴⁾ in October of 1995. Listed in table 1(a) are the relevant data that he has provided for the combination magnet parameters and in table 1(b) for the phase space parameters and the matrix elements for the fringe fields.

2.2 Starting Point of the Beam line

One further difference between the original configuration of the beam line and that considered here is that the combination magnet has been rotated 4° counter-clockwise in the present design (fig. 2) from its location in the original design (fig. 1). Extraction studies track the extracted beam from the stripper foil to a point well beyond the (effective) edge of the combination magnet. Consequently, it is necessary to determine that location in order to specify the location of the components of the beam line.

The upper portion of figure 3 shows the trajectories of the extracted beam as calculated by R Lee. It shows that the crossover point of the combination magnet is located at an (R, θ) coordinate of (412.32 inches, 327.00°) with respect to the centerline of valley 3. Consequently, the radius vector makes an angle of (29°

$+ 327^\circ - 360^\circ) = -4.0^\circ$ with respect to the positive x -axis of this report. In this coordinate system then, the crossover point is located at the coordinates

$$\begin{aligned}(x_{co}, y_{co}) &= (412.32 \cos(-4.0^\circ), 412.32 \sin(-4.0^\circ)) \text{ inches} \\ &= (411.315609, -28.761989) \text{ inches} \\ &= (10.447417, -0.730555) \text{ m.}\end{aligned}$$

Recalling that the effective length of the magnet has been taken as 13.78 inches (0.35 m) and assuming that the crossover point is at the center of the magnet, we then calculate the distance from there to the magnet edge as

$$\begin{aligned}(\delta x, \delta y) &= (6.89 \cos(35.0^\circ), 6.89 \sin(35.0^\circ)) \text{ inches} \\ &= (5.643958, 3.951942) \text{ inches} \\ &= (0.143357, 0.100379) \text{ m.}\end{aligned}$$

Thus the exit edge of the magnet is located at

$$\begin{aligned}x_{magexit} &= x_{co} + \delta x \\ &= 10.447417 + 0.143357 \text{ m} \\ &= 10.590774 \text{ m}\end{aligned}$$

and

$$\begin{aligned}y_{magexit} &= y_{co} + \delta y \\ &= -0.730555 + 0.100379 \text{ m} \\ &= -0.630176 \text{ m.}\end{aligned}$$

From the work of R. Lee we find that at 489.466 MeV the tracing done to generate the fringe-field transfer matrices ends at an $(R_{traj}, \theta_{traj}) = (436.345 \text{ inches}, 329.511^\circ)$. Thus, in the (x, y) system used here, the extracted trajectory makes an angle with respect to the positive x -axis of $(29^\circ + 329.511^\circ - 360^\circ) = -1.489^\circ$ and the end of the fringe-field calculation becomes

$$\begin{aligned}(x_{traj}, y_{traj}) &= (436.345 \cos(-1.489^\circ), 436.345 \sin(-1.489^\circ)) \text{ inches} \\ &= (436.197660, -11.338437) \text{ inches} \\ &= (11.079421, -0.287996) \text{ m.}\end{aligned}$$

Thus we must back up a distance

$$\begin{aligned}\Delta_{490} &= \sqrt{(x_{traj} - x_{magexit})^2 + (y_{traj} - y_{magexit})^2} \\ &= \sqrt{(11.079421 - 10.590774)^2 + (-0.287996 - (-0.630176))^2} \\ &= \sqrt{0.488647^2 + 0.342180^2} \\ &= 0.596543 \text{ m}\end{aligned}$$

along the exiting trajectory to reach the magnet exit. Similar calculations at an energy of 499.456 MeV [end-point $(R_{traj}, \theta_{traj}) = (436.169 \text{ in.}, 329.493^\circ)$] and 479.477 MeV [end-point $(R_{traj}, \theta_{traj}) = (436.498 \text{ in.}, 329.526^\circ)$] yield values of $\Delta_{500} = 0.590696 \text{ m}$ and $\Delta_{480} = 0.601392 \text{ m}$ respectively. We average these to obtain the average back-up distance

$$\Delta_{av} = 0.596210 \text{ m.}$$

In the TRANSPORT calculations presented here, a back-up distance of 0.59617 m was used (in error). However, the 0.4 mm error introduced will have no effect on the calculations.

3. Beam Line Design

3.1 General Considerations

The design philosophy followed in ref⁴⁾—the production of a parallel beam and a double waist within the vault followed by a series of repeating unit sections, thus reproducing the original waist at successive points along the beam line—was abandoned because REVMOC studies indicated excessive beam spill along the line. These spills were predicted to occur in the vertical plane because, at the point of stripping, the vertical beam divergence is small and foil scattering dominates the divergence of the unstripped beam. Consequently, instead of the scheme shown in figure 1, that shown in figure 2 was adapted. We note again that in each of these figures the cyclotron center is taken as $(x, y) = (0,0)$.

A TRANSPORT listing for a 500 MeV case is given in table 2. Figure 4 shows the beam envelopes along the beam line; only those for 490 and 500 MeV are shown because the 480 MeV envelopes are indistinguishable from those of the 490 MeV tune. (In future plots of beam envelopes, this procedure will be maintained.) The small ‘tail’ that appears in this plot at the beginning of the beam line results because of the back up to the effective exit of the combination magnet that is required.

3.2 Vault Section

A quadrupole doublet is located downstream of the combination magnet and upstream of the first of two 27.5° dipoles and a second doublet is positioned downstream of the second dipole. These doublets are used to control the vertical beam height in the dipoles and to produce a double waist at the point labelled WST1. In addition, a beam size of $(\pm x, \pm y) = (\pm 1.1, \pm 0.66)$ cm is required here.

The first doublet is composed of two of the standard TRIUMF 4Q14/8 quadrupoles. Those of the second doublet are of a new TRIUMF design⁵⁾, modified as suggested by A. Otter⁶⁾, and are akin to the TRIUMF 4Q9/8 quadrupoles that were purchased from Alpha Magnetics some time ago. These new quadrupoles will be designated as TRIUMF type 4Q8/8 throughout this report.

A triplet of 4Q8/8 quadrupoles just inside the north wall of the vault is used to produce a double waist 8 m beyond the outer of the vault wall.

Figure 5 shows an enlarged view of the beam-transport elements that lie within the cyclotron vault proper. In addition, the beam envelopes for this section of beam line are also shown. The tail resulting from backing up to the combination magnet exit is obvious in this figure.

3.3 WST1 to WST3 Section

This section carries the beam through the vault wall and is shown in an enlarged view in figure 6. The figure also shows the beam envelopes in this section of beam line. Components of this section are the vault quadrupole triplet 2AVQ5/6/7 and a second triplet 2AQ8/9/10.

As noted above, the 2AVQ5/6/7 triplet produce a double waist at the location labelled WST2, 8 m from the external wall of the vault. The 2AQ8/9/10 triplet, consisting of 4Q14/8 quadrupoles, produces another waist at the location labelled WST3. These two triplets are tuned to keep the vertical size of the beam small and to produce a vertical beam size of ± 0.291 cm at WST3.

3.4 WST3 to Target Section

This section is composed of quadrupole doublets 2AQ11/12 and 2AQ13/14, quadrupole singlets 2AQ15 and 2AQ16, a $\pm 15^\circ$ switching magnet 2AB3 and a 15° dipole 2AB4. All quadrupoles are of the 4Q8/8 variety. The first doublet produces a double waist at location WST4 and the remaining quadrupoles are used to produce the required beam size at the target location and, at the same time, to produce a spatially achromatic beam spot ($R_{16} = 0$) there. The redundancy of quadrupoles allows the control of the vertical

beam size in the dipoles should such be required.

Beam profiles and an expanded view of this section of beam line are shown figure 7. A nominal beam size at the target of $(\pm x, \pm y) = (\pm 0.25, \pm 0.25)$ cm is the design goal.

4. Settings of the beam-transport elements

Table 3 lists the settings of the various elements of the transport system for the energy range 480, 490 and 500 MeV. In table 4 we list the beam sizes at the various waist locations.

Beam sizes and overall transfer matrices at the TGT2 location are listed in table 5(a); those at the TGT1 location are listed in table 5(b).

5. REVMOC calculations

The program REVMOC⁷⁾ was run at all energies to estimate the amount of beam spill to be expected and where such might occur. REVMOC is a Monte Carlo program that traces particles through a beam optics configuration using true second-order optics, although the effects of chromatic aberrations is considered to all orders. The effects of multiple scattering, decay, nuclear scattering and energy loss in scatterers, absorbers, collimators, slits and apertures are included. Geometric effects are considered locally to only second order but higher-order global effects will appear because of the accumulation of the second-order effects. The program does not, however, optimize beam elements and its primary use is to do detailed checks on a beam line that has been designed using the program TRANSPORT⁸⁾.

For each energy and each target configuration 150,000 particles (in some cases, 1,500,000 particles) were traced through the beam line. At 500 and 490 MeV a spill of 0.013% of the beam was predicted to be lost between the stripper foil and the combination magnet exit; at 480 MeV a spill of 0.009% was predicted in the same region. No beam was predicted to be spilled elsewhere in the beam line. All spill was predicted to occur in the vertical plane.

The reason for spill in the vertical plane only is shown in figure 8, a plot of the vertical divergence (DY) in mr along the vertical axis versus the vertical beam size (Y) in cm along the horizontal axis at the WST1 location. The upper portion of the plot is a prediction of this correlation *without* any foil scattering taken into account; the lower portion is the prediction taking into account the scattering in a carbon stripper foil that is 0.00003 m (0.0012 in.) thick. It is clear that the foil scattering adds significantly to the beam divergence. The reason for this, as discussed in section 3.1, is the extremely low vertical divergence of the beam at the point of stripping.

Figure 9 shows the predicted beam spot at the TGT2 target location for a beam energy of 500 MeV. Again, the upper portions of the figure show the predicted spot size without foil scattering and the lower portion that including foil scattering. The units of the vertical and horizontal scales are cm. It is clear that a significant increase in spot size can be attributed to foil scattering. Figure 10 is a density plot of the same data.

Figures 11 and 12 are similar plots for a beam energy of 490 MeV and figures 13 and 14 those for a beam energy of 480 MeV.

Using the data presented in figure 9, we find that REVMOC predicts that 2.65% (11.06%) of the beam lies *outside* the nominal design spot size of ± 0.26 cm in the horizontal (vertical) plane at a beam energy of 500 MeV. At 490 and 480 MeV the corresponding values are 2.64% (12.47 %) and 2.63% (11.82%) respectively. 0.02% (1.87%) of the beam is predicted to lie outside of a ± 0.42 cm diameter in the horizontal (vertical) plane at 500 MeV, with corresponding values of 0.02% (2.05%) and 0.01% (1.75%), respectively, at energies of 490 and 480 MeV. Less than 0.01% of the beam is predicted to lie outside of ± 0.60 cm in the horizontal

plane at all energies. In the vertical plane 0.69% of the beam is predicted to lie outside of ± 0.60 cm at 500 MeV with corresponding values of 0.71% and 0.58%, respectively, at energies of 490 and 480 MeV.

Finally, figure 15 shows a plot of momentum p in GeV/c along the vertical axis versus horizontal position x in cm along the horizontal axis at the TGT2 location. That momentum and horizontal position are uncorrelated indicates that the beam is spatially achromatic there. Similar plots for 490 and 480 MeV show the same property.

6. Discussion

Since a proposal for an ISAC facility was first made, many versions of its beam transport line have been considered. This report presents the results of a design for the final version of that beam line.

Extraction matrices have been produced for energies of 480, 490 and 500 MeV and beam-line optics for these energies have been developed. In addition, beam spill calculations were made. These indicated that beam spill should be contained within the cyclotron vault.

It should be noted, however, that the accuracy to which the program REVMOC was asked to predict beam spill is, at best, at the limit of the program. In normal use, one would expect an accuracy of 0.5% at best. Thus the quoted beam spills should be regarded as indications that spill might occur rather than an absolute value to be quoted.

References

1. G. M. Stinson, *TRIUMF report* TRI-DNA-95-2, TRIUMF, 1995.
2. G. M. Stinson, *TRIUMF report* TRI-DNA-95-8, TRIUMF, 1995. ***
3. C. J. Kost, *TRIUMF report* TRI-DN-82-17, TRIUMF, 1982.
4. R. Lee, *Private communication*, TRIUMF, October, 1995.
5. G. M. Stinson, *TRIUMF report* TRI-DNA-96-7, TRIUMF, 1996.
6. A. J. Otter, *Private communication*, TRIUMF, June, 1996.
7. C. J. Kost and P. A. Reeve, *TRIUMF report* TRI-DN-82-28, TRIUMF, 1982.
8. K. L. Brown and S. K. Howry, *TRANSPORT/360*, SLAC-91, Stanford Linear Accelerator Laboratory, July, 1970.

*** This report was never issued.

Table 1 (a)
Combination magnet parameters from ref⁴⁾

Parameter	480 MeV	490 MeV	500 MeV
Entry angle (°)	-0.977	-0.138	0.687
Field (kG)	1.726	0.248	-1.245
Exit angle (°)	0.000	0.000	0.000
Bend angle (°)	-0.977	-0.138	0.687

Table 1 (b)
Fringe field and initial beam parameters from ref⁴⁾

Parameter	480 MeV	490 MeV	500 MeV
$\pm x$ (cm)	0.127	0.127	0.127
$\pm \theta$ (mr)	1.600	1.600	1.600
$\pm y$ (cm)	0.669	0.669	0.669
$\pm \phi$ (mr)	0.556	0.556	0.556
R_{11} (cm/cm)	-0.03099	-0.01551	-0.06571
R_{12} (cm/mr)	0.32538	0.32610	0.32167
R_{16} (cm/%)	1.36150	1.32879	1.28344
R_{21} (mr/cm)	-3.09350	-3.06770	-3.17670
R_{22} (mr/mr)	0.16141	0.17049	0.16907
R_{26} (mr/%)	2.38040	2.43140	2.45410
R_{33} (cm/cm)	1.12700	1.11600	1.10800
R_{34} (mr/cm)	0.61980	0.61590	0.61200
R_{43} (mr/cm)	0.48200	0.46410	0.44710
R_{44} (cm/cm)	1.15300	1.15300	1.14900

Coordinates of the cross-over point of the combination magnet are:

$$R = 412.320 \text{ inches}$$

$$\theta = 327.000^\circ \text{ with respect to the centerline of valley 3}$$

Table 3

TRANSPORT listing for beam line 2A at 500 MeV

'DATA OF 95/10/10 - 500 MEV ON LINE 2-A - TGT2 - DOUBLE WAIST AT WST1'

0

13.00	', '	12.00000;			
16.00	'1/R1'	12.00000	0.00000;		
16.00	'1/R2'	13.00000	0.00000;		
16.00	'G/2 '	5.00000	5.08000;		
16.00	'X0 '	16.00000	-0.29135;		
16.00	'Z0 '	18.00000	11.07463;		
16.00	'T0 '	19.00000	35.10000;		
1.00	'BEAM'	0.12700	1.60000	0.66900	0.55600
		0.00000	0.10000	1.09007;	
12.00	'12 '	0.00000	0.00000	0.00000	0.00000
		0.00000	-0.96300	0.00000	0.00000
		0.00000	0.00000	0.00000	0.00000
		0.00000	0.00000	0.00000;	
1.00	'FOIL'	0.00000	0.17100	0.00000	0.17100
		0.00000	0.00000	0.00000	0.00000
14.00	'R1 '	-0.06571	0.32167	0.00000	0.00000
		0.00000	1.28344	1.00000;	
14.00	'R2 '	-3.17670	0.16907	0.00000	0.00000
		0.00000	2.45410	2.00000;	
14.00	'R3 '	0.00000	0.00000	1.10800	0.61200
		0.00000	0.00000	3.00000;	
14.00	'R4 '	0.00000	0.00000	0.44710	1.14900
		0.00000	0.00000	4.00000;	
3.00	'CMEX'	-0.59617;			
3.00	', '	0.21004;			
3.00	', '	0.30940;			
5.00	'2VQ1'	0.40900	-3.65811	5.08000;	
3.00	', '	0.25000;			
5.00	'2VQ2'	0.40900	5.24015	5.08000;	
3.00	', '	0.23880;			
3.00	'B1IN'	0.37190;			
20.00	', '	180.00000;			
2.00	', '	13.75000;			
4.00	'BEN1'	1.24595	14.00681	0.00000;	
2.00	', '	13.75000;			
20.00	', '	-180.00000;			
3.00	'B1EX'	0.00001;			
3.00	', '	0.08972;			
3.00	', '	0.27380;			
3.00	', '	0.52450;			
3.00	', '	0.27380;			

Table 3 (continued)

3.00	'B2IN'	0.08972;			
20.00	', '	180.00000;			
2.00	', '	13.75000;			
4.00	'BEN2'	1.24595	14.00681	0.00000;	
2.00	', '	13.75000;			
20.00	', '	-180.00000;			
3.00	'B2EX'	0.00001;			
-10.00	'ZFIT'	8.00000	3.00000	14.07160	0.00100;
3.00	', '	1.00000;			
5.00	'2VQ3'	0.26600	5.61565	5.08000;	
3.00	', '	0.28640;			
5.00	'2VQ4'	0.26600	-4.61145	5.08000;	
3.00	', '	0.40900;			
3.00	', '	0.28640;			
3.00	', '	1.00000;			
3.00	', '	1.00000;			
3.00	'WST1'	1.78321;			
-10.00	'FXW1'	2.00000	1.00000	0.00000	0.00100;
-10.00	'FYW1'	4.00000	3.00000	0.00000	0.00100;
-10.00	'SXW1'	1.00000	1.00000	1.15000	0.01000;
-10.00	'SYW1'	3.00000	3.00000	0.66000	0.01000;
3.00	', '	1.00000;			
3.00	', '	1.23290;			
5.00	'2VQ5'	0.26600	-1.63667	5.08000;	
3.00	', '	0.28640;			
5.00	'2VQ6'	0.26600	3.07293	5.08000;	
3.00	', '	0.28640;			
5.00	'2VQ7'	0.26600	-1.63667	5.08000;	
3.00	', '	0.95770;			
3.00	'WALL'	1.51760;			
-10.00	'ZFIT'	8.00000	1.00000	15.24000	0.00100;
3.00	'MID2'	0.92100;			
3.00	'WALX'	1.36500;			
3.00	', '	1.00000;			
3.00	', '	1.00000;			
3.00	', '	1.00000;			
3.00	', '	1.00000;			
3.00	', '	1.00000;			
3.00	', '	1.00000;			
3.00	', '	1.00000;			
3.00	'WST2'	1.00000;			
-10.00	'FXW2'	2.00000	1.00000	0.00000	0.00100;
-10.00	'FYW2'	4.00000	3.00000	0.00000	0.00100;
3.00	', '	1.00000;			
3.00	', '	1.00000;			

Table 3 (continued)

3.00	''	1.00000;		
5.00	'AQ8'	0.40900	-1.52377	5.08000;
3.00	''	0.30480;		
5.00	'AQ9'	0.40900	2.63564	5.08000;
3.00	''	0.30480;		
5.00	'AQ10'	0.40900	-1.52377	5.08000;
3.00	''	0.96066;		
3.00	''	0.96066;		
3.00	''	1.04211;		
3.00	'WST3'	0.60000;		
-10.00	'FXW3'	2.00000	1.00000	0.00000 0.00100;
-10.00	'FYW3'	4.00000	3.00000	0.00000 0.00100;
-10.00	'SYW3'	3.00000	3.00000	0.29100 0.00500;
3.00	''	1.00000;		
3.00	''	1.00000;		
3.00	''	1.13330;		
5.00	'AQ11'	0.26600	2.32290	5.08000;
3.00	''	0.28640;		
5.00	'AQ12'	0.26600	-2.62885	5.08000;
3.00	''	1.13330;		
3.00	''	1.00000;		
3.00	'WST4'	1.00000;		
3.00	''	1.08328;		
3.00	''	1.08328;		
3.00	''	1.08328;		
3.00	''	1.07408;		
5.00	'AQ13'	0.26600	4.68356	5.08000;
3.00	''	0.28640;		
5.00	'AQ14'	0.26060	-5.95294	5.08000;
3.00	''	1.07408;		
3.00	''	1.08328;		
3.00	''	1.08328;		
3.00	'B3IN'	1.08328;		
16.00	'1/R2'	13.00000	1.73055;	
20.00	''	180.00000;		
2.00	''	0.00000;		
4.00	'BEN3'	0.68139	13.97007	0.00000;
2.00	''	0.00000;		
20.00	''	-180.00000;		
3.00	'B3EX'	0.00001;	3.00	'' 0.75000;
3.00	''	0.74200;		
5.00	'AQ15'	0.26600	-3.89857	5.08000;
3.00	'B4IN'	0.49200;		
16.00	'1/R2'	13.00000	0.00000;	
20.00	''	180.00000;		

Table 3 (continued)

2.00	''	7.50000;			
4.00	'BEN4'	0.68139	13.97007	0.00000;	
2.00	''	7.50000;			
20.00	''	-180.00000;			
3.00	'B4EX'	0.00001;	3.00	''	0.26500;
3.00	''	0.26500;			
3.00	''	0.25580;			
5.00	'AQ16'	0.26600	4.21714	5.08000;	
3.00	''	0.87457;			
3.00	''	0.88377;			
3.00	''	0.88377;			
3.00	'TGT2'	0.88377;			
-10.00	''	-1.00000	6.00000	0.06000	0.00100;
-10.00	''	1.00000	1.00000	0.25000	0.01000;
-10.00	''	3.00000	3.00000	0.25000	0.01000;
-10.00	'ZFIT'	8.00000	1.00000	57.91640	0.00100;
-10.00	'ZFIT'	8.00000	3.00000	10.85215	0.00100;

Table 4
Element settings as a function of energy for beam line 2A

Element	Field (kG) at energy					
	480 MeV	490 MeV	500 MeV			
2AVQ1	-3.55885	-3.59340	-3.63609			
2AVQ2	5.03422	5.09663	5.21560			
2AVB1	13.66610	13.83687	14.00681			
2AVB2	13.66610	13.83687	14.00681			
2AVQ3	5.53312	5.59629	5.61565			
2AVQ4	-4.54074	-4.58767	-4.60155			
2AVQ5	-1.59219	-1.61331	-1.66483			
2AVQ6	2.99027	3.03033	3.12057			
2AVQ7	-1.59219	-1.61331	-1.66483			
2AQ8	-1.47043	-1.49054	-1.52363			
2VQ9	2.54777	2.58248	2.63611			
2Q10	-1.47043	-1.49054	-1.52363			
2AQ11	2.25242	2.28376	2.32602			
2AQ12	-2.54611	-2.58129	-2.63114			
2AQ13 ^{a)}	4.61772	4.79248	4.64310	4.81992	4.67409	4.87956
2AQ14 ^{a)}	-5.95294	-5.94608	-5.95294	-5.94570	-5.95294	-5.99002
2AB3	13.63020		13.80052		13.97007	
2AQ15 ^{a)}	-3.76199	-3.81598	-3.83138	-3.86877	-3.89720	-3.90365
2AB4	13.63020		13.80052		13.97007	
2AQ16 ^{a)}	4.10900	4.21635	4.16444	4.26979	4.21185	4.31154

^{a)} Two field values are listed for quadrupoles 2AQ13 through 2AQ16. At a given energy, the left value refers to beam delivery to the target labelled TGT2 and the right to beam delivery to that labelled TGT1.

Table 5
Beam sizes at the waist locations

Waist	Parameter	480 MeV	490 MeV	500 MeV
WST1	$\pm x$ (cm)	1.150	1.150	1.182
	$\pm \theta$ (mr)	0.354	0.355	0.364
	$\pm y$ (cm)	0.660	0.660	0.661
	$\pm \phi$ (mr)	0.231	0.231	0.230
WST2	$\pm x$ (cm)	1.050	1.049	1.079
	$\pm \theta$ (mr)	0.387	0.389	0.339
	$\pm y$ (cm)	0.332	0.332	0.329
	$\pm \phi$ (mr)	0.459	0.459	0.461
WST3	$\pm x$ (cm)	1.047	1.046	1.076
	$\pm \theta$ (mr)	0.389	0.390	0.400
	$\pm y$ (cm)	0.294	0.293	0.291
	$\pm \phi$ (mr)	0.518	0.519	0.522
WST4	$\pm x$ (cm)	0.853	0.851	0.875
	$\pm \theta$ (mr)	0.477	0.479	0.492
	$\pm y$ (cm)	0.397	0.397	0.397
	$\pm \phi$ (mr)	0.383	0.383	0.383

Table 6(a)

Beam sizes and overall transfer matrices at the TGT2 location

Parameter	480 MeV	490 MeV	500 MeV
$\pm x$ (cm)	0.250	0.250	0.250
$\pm \theta$ (mr)	3.417	3.423	2.374
$\pm y$ (cm)	0.250	0.250	0.250
$\pm \phi$ (mr)	1.099	1.047	2.225
R_{11} (cm/cm)	-0.8329	-0.8233	-0.7662
R_{12} (cm/mr)	-0.1408	-0.1411	-0.1431
R_{16} (cm/%)	0.0000	0.0000	0.0000
R_{21} (mr/cm)	-5.1879	-5.0881	-4.3150
R_{22} (mr/mr)	-2.0793	-2.0841	-2.1250
R_{26} (mr/%)	-2.1669	-2.2470	3.2756
R_{33} (cm/cm)	-0.3508	-0.4335	-0.5182
R_{34} (mr/cm)	-0.7712	-0.8419	-0.9101
R_{43} (mr/cm)	0.8818	0.6001	0.3431
R_{44} (cm/cm)	-0.9143	-1.1435	-1.3261

Table 6(b)

Beam sizes and overall transfer matrices at the TGT1 location

Parameter	480 MeV	490 MeV	500 MeV
$\pm x$ (cm)	0.250	0.250	0.250
$\pm \theta$ (mr)	3.882	3.887	3.995
$\pm y$ (cm)	0.250	0.250	0.250
$\pm \phi$ (mr)	0.993	0.913	0.853
R_{11} (cm/cm)	-0.3708	-0.3660	-0.3086
R_{12} (cm/mr)	-0.1526	-0.1527	-0.1513
R_{16} (cm/%)	0.0004	0.0003	0.0003
R_{21} (mr/cm)	1.9589	1.9939	2.7292
R_{22} (mr/mr)	-1.8945	-1.8942	-1.9179
R_{26} (mr/%)	-23.9101	-23.9869	-25.1329
R_{33} (cm/cm)	-0.5131	-0.6445	-0.7253
R_{34} (mr/cm)	-0.9095	-1.0003	-1.0502
R_{43} (mr/cm)	0.3556	-0.0319	-0.2198
R_{44} (cm/cm)	-1.3223	-1.6025	-1.6964

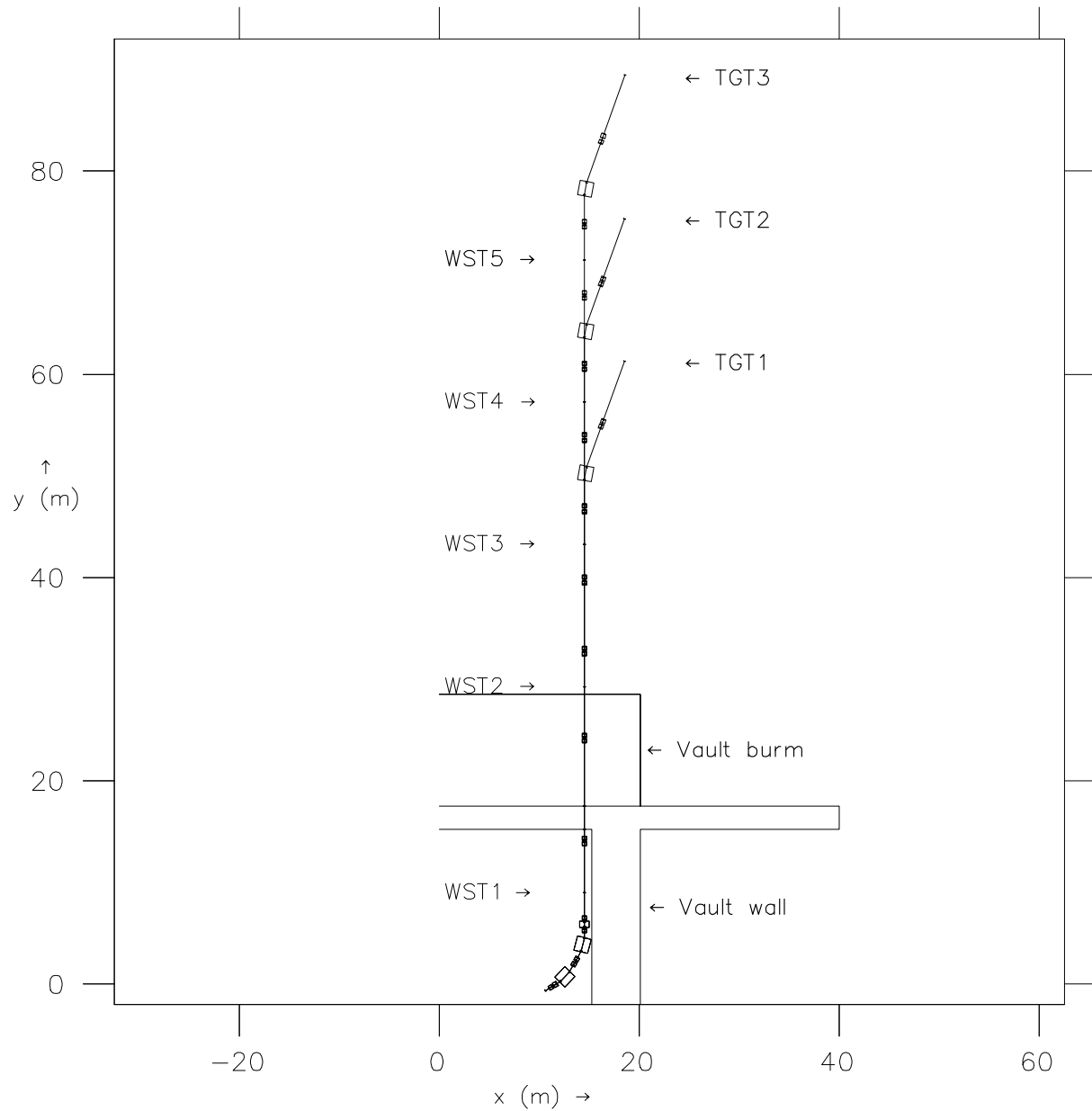


Figure 1. The original configuration of beam line 2A.

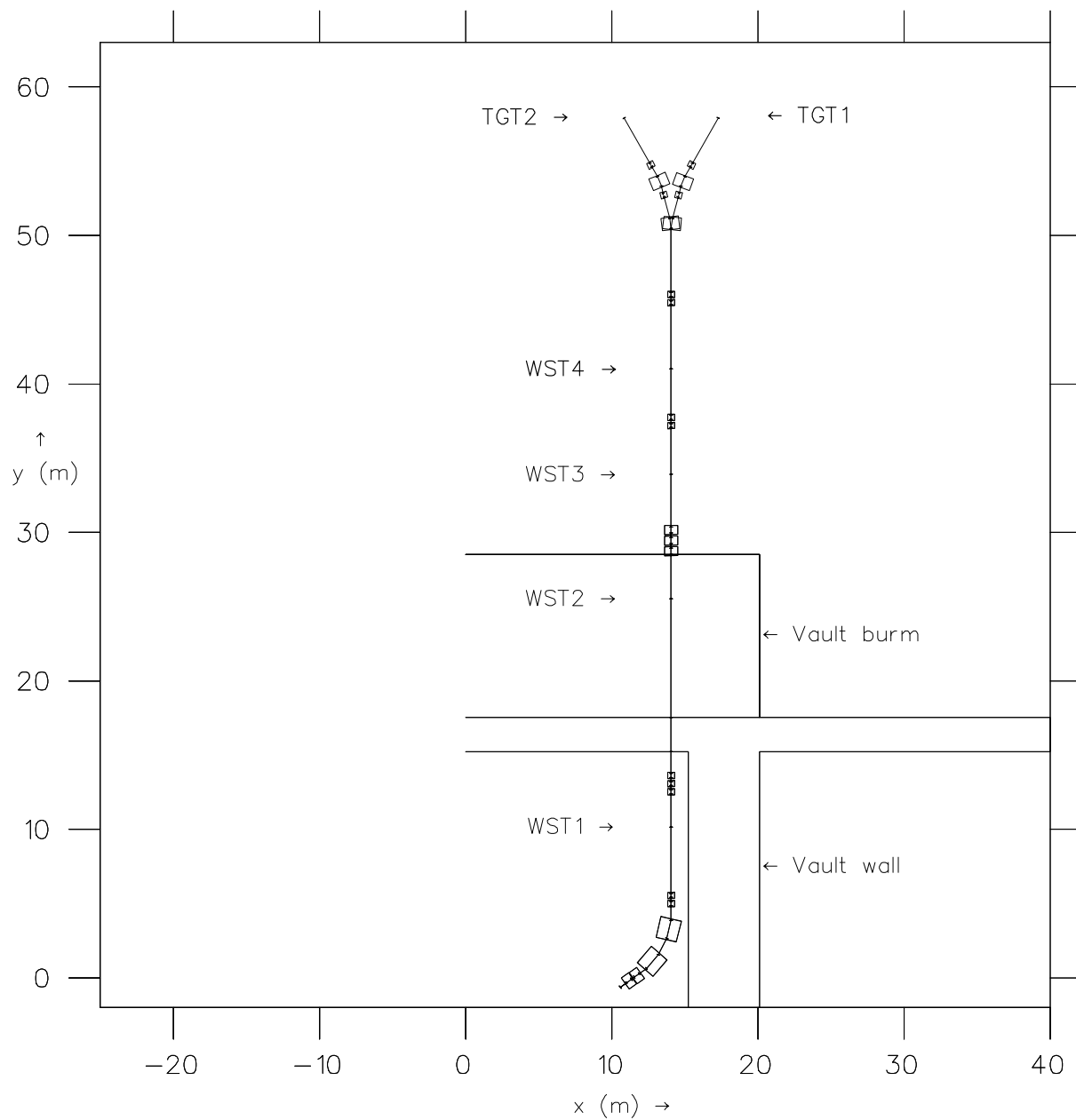


Figure 2. The proposed configuration of beam line 2A.

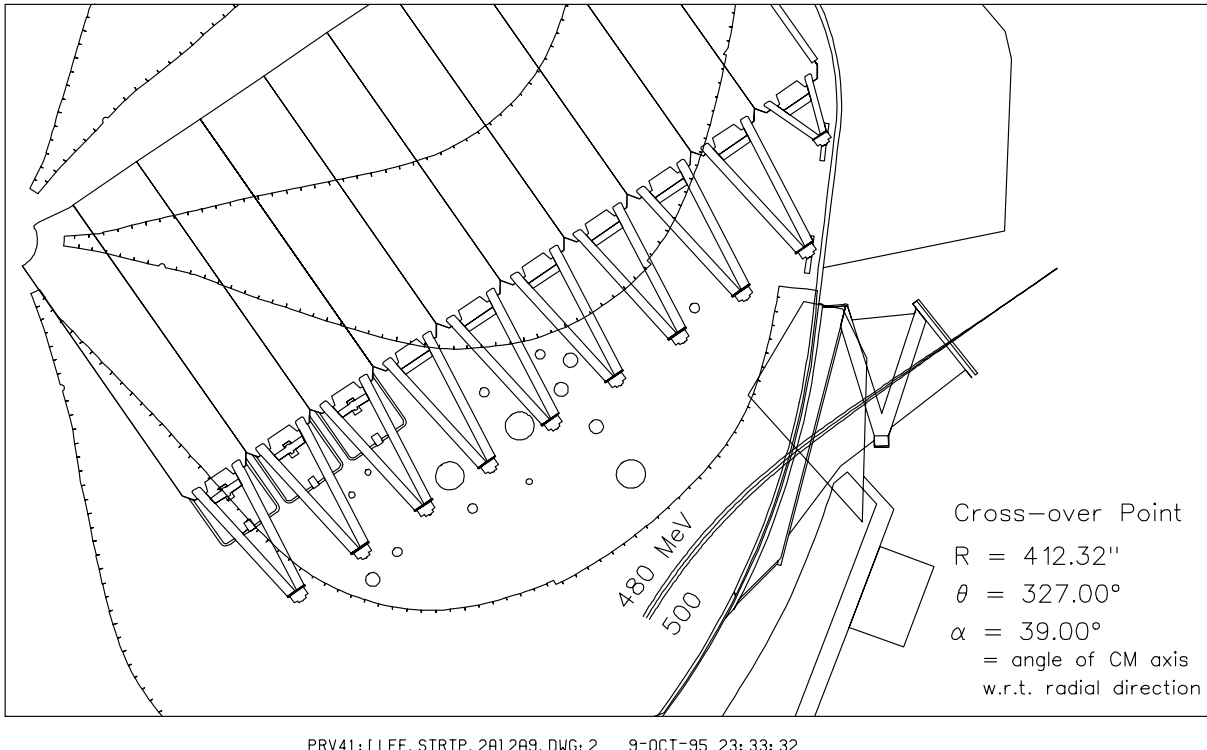


figure 3(a). The extraction trajectories for energies of 480, 490 and 500 MeV.

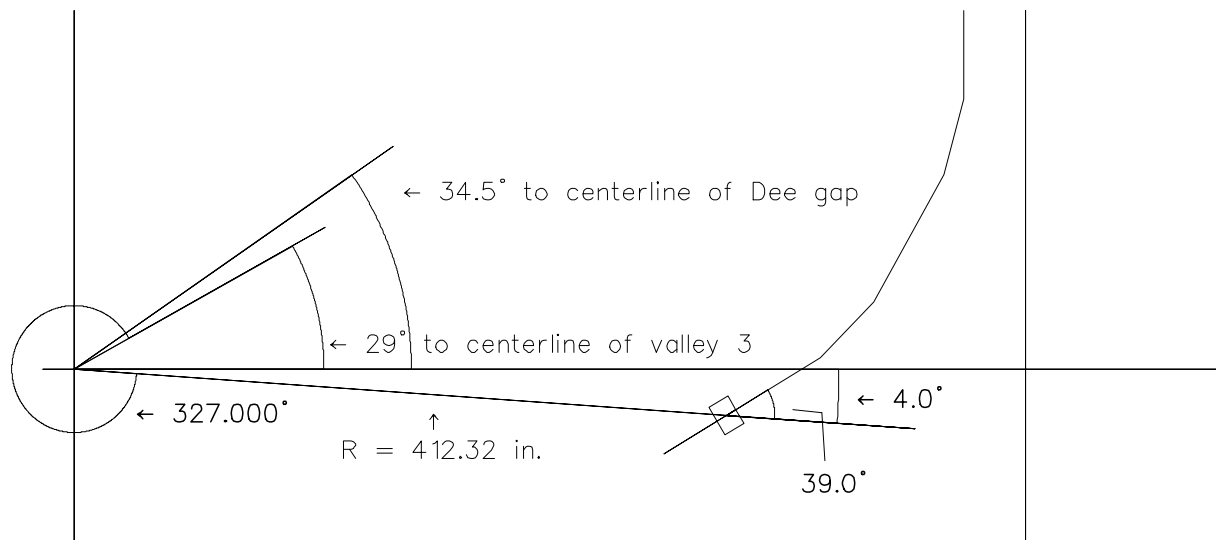


Figure 3(b). The essential geometry of beam line 2A extraction.

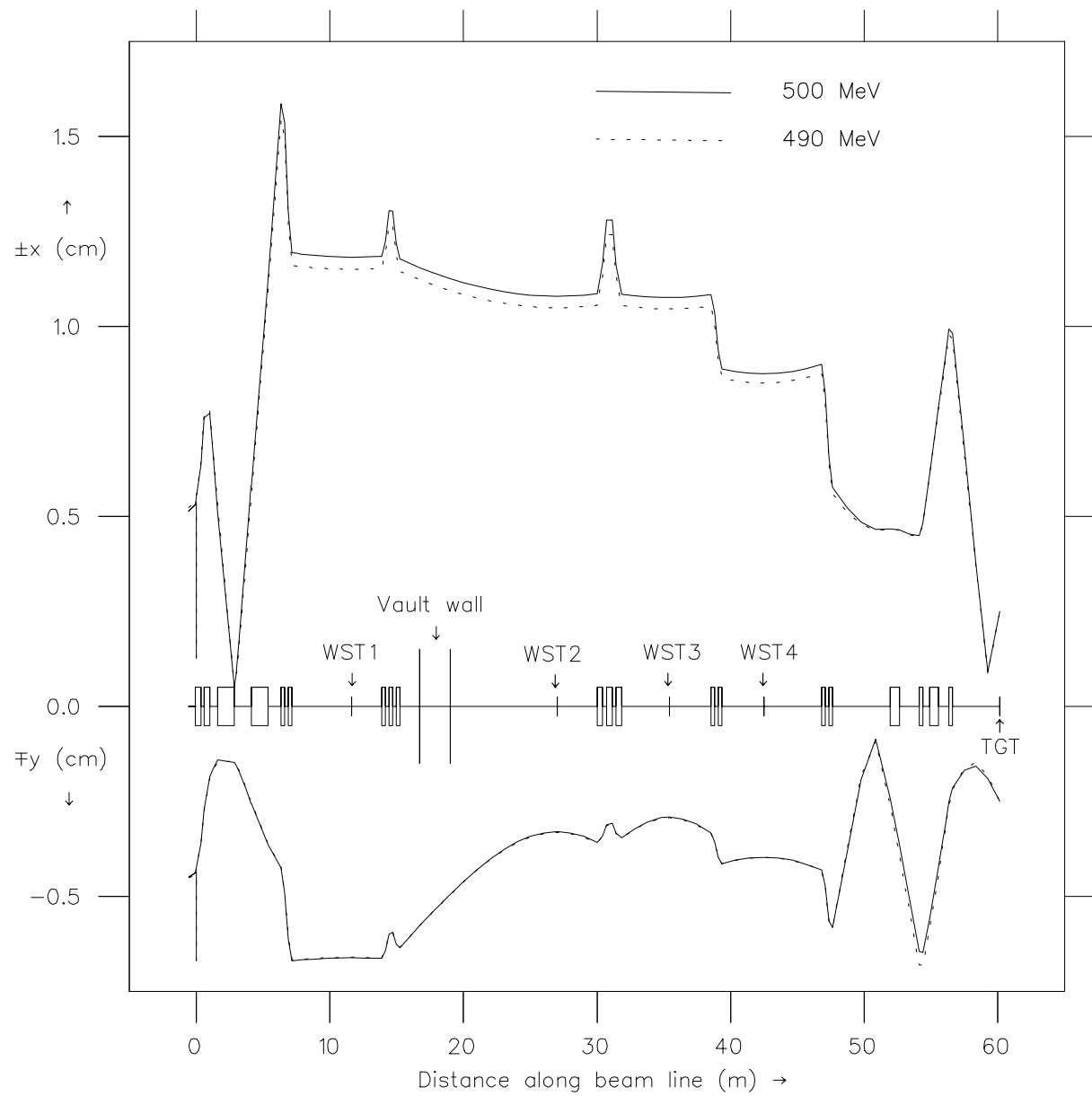


Figure 4. Beam envelopes along beam line 2A.

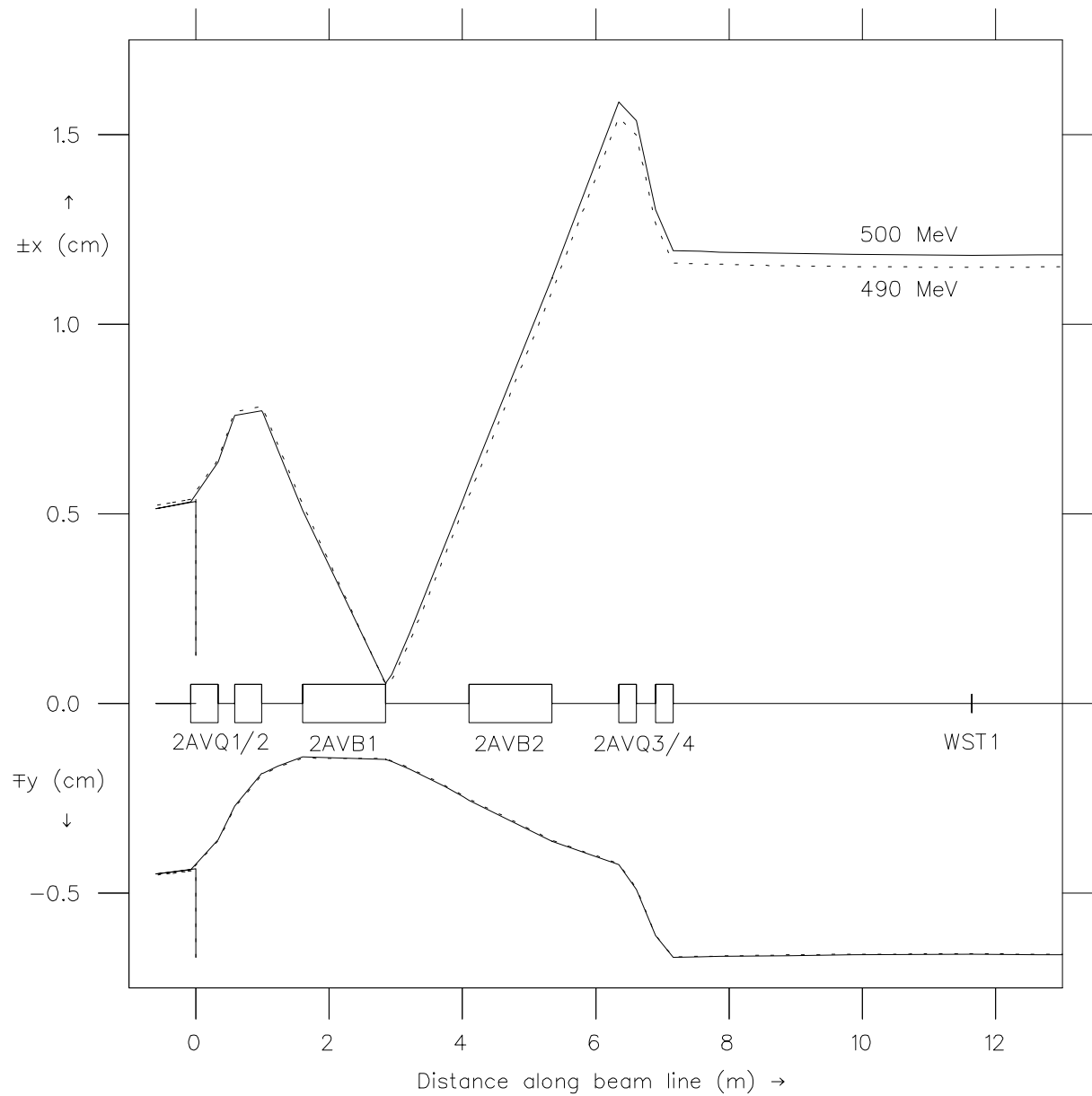


Figure 5. Beam envelopes in the vault section of beam line 2A.

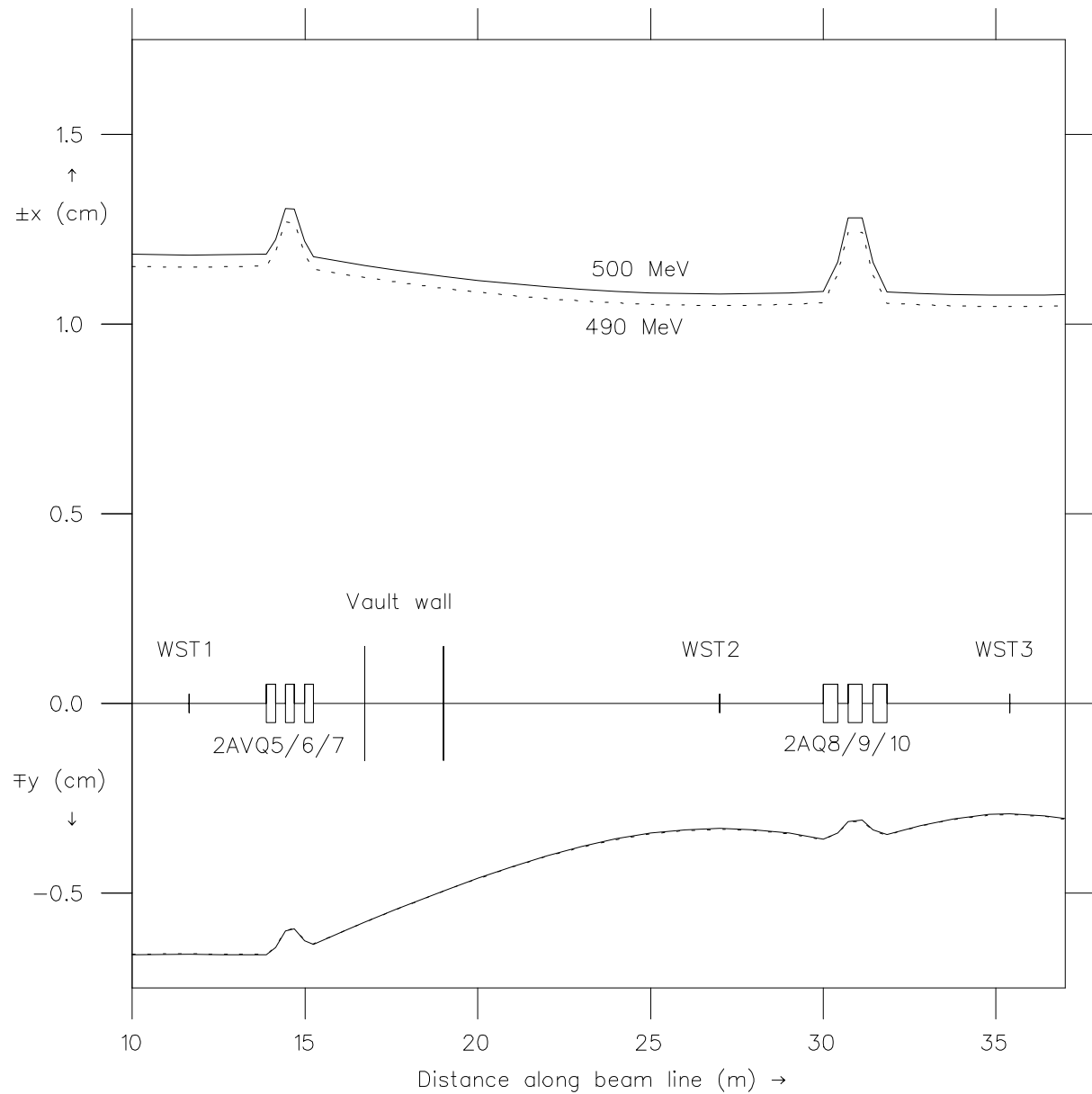


Figure 6. Beam profiles between WST1 and WST3 locations on beam line 2A.

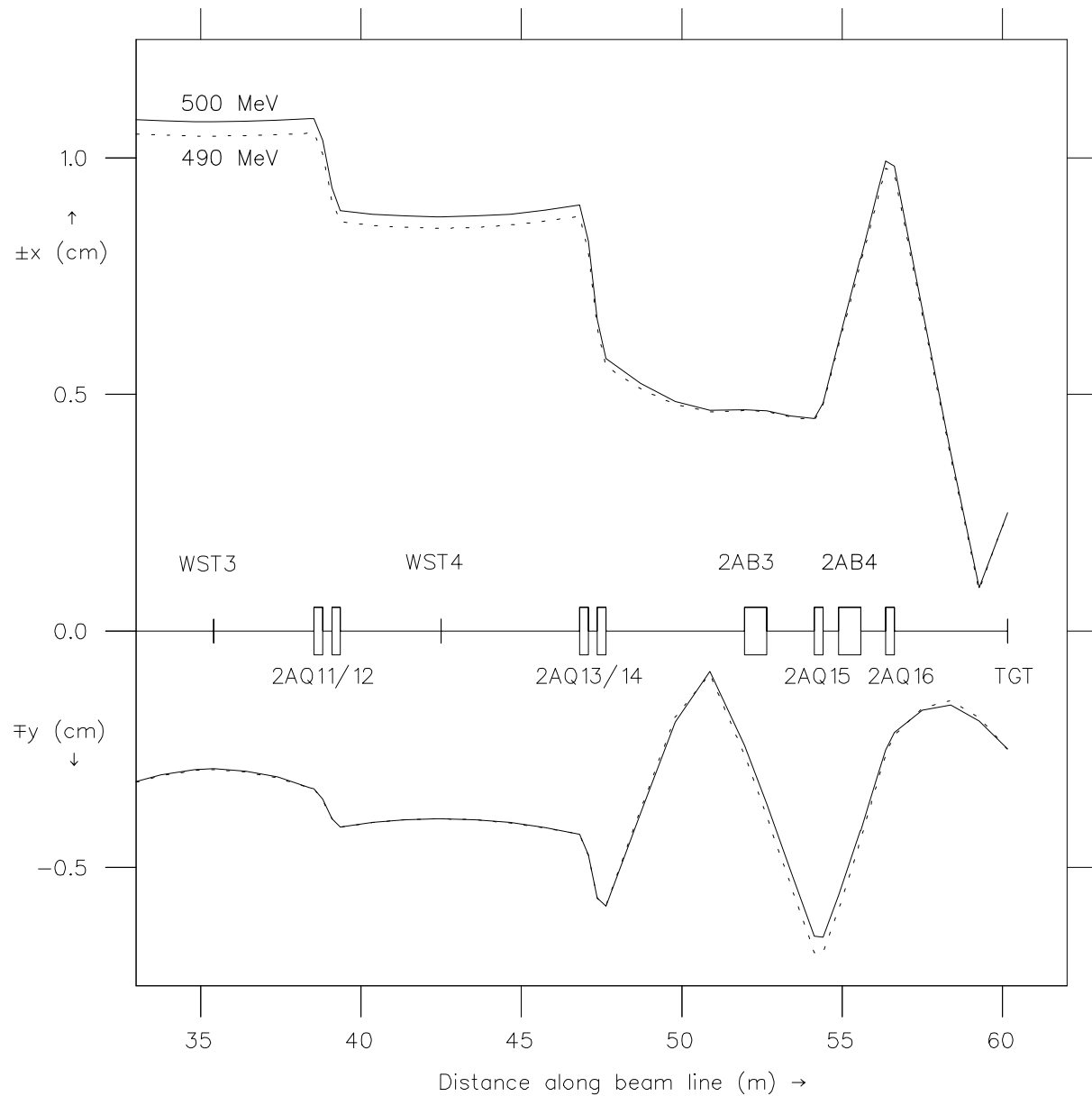


Figure 7. Beam profiles in the WST3 to TGT2 section of beam line 2A.

DATA OF 95/10/10 ON 96/06/25 - 500 MEV ON 2-A - NEW TRIPLETS - 2xWst @ WST1 - TGT2

Space # 8: Distribution of particles as a function of X AT TGT2 (Element #146) (along HORIZONTAL axis)
 & Y at TGT2 (Element #146) (along VERTICAL axis)

Distribution of particles INITIALLY ACCEPTED
 COUNTS = 150000.
 X PROJECTION

1.105	0
Y 0.9350	0 Y
0.7650	0
0.5950	0 P
A 0.4250	0 R
T 0.2550	44 0
0.8500E-01	2 59284715*****764305 47 1 31488 J
T - .8500E-01	2139836*****807120 1 86850 E
G - .2550	1 61261707*****788285 43 31582 C
T - .4250	36 T
2 - .5950	0 I
- .7650	0 O
- .9350	0 N
-1.105	0
X AT TGT2	

REAL! Distribution of FINAL RUN FOUND HERE
 COUNTS = 149981.
 X PROJECTION

2.465	7
2.295	5
2.125	3
1.955	9
1.785	7
1.615	14
1.445	14
1.275	20
1.105	27
Y 0.9350	46 Y
0.7650	112
0.5950	225 P
A 0.4250	874 R
T 0.2550	6944 0
0.8500E-01	35422 J
T - .8500E-01	62313 E
G - .2550	35652 C
T - .4250	6844 T
2 - .5950	899 I
- .7650	267 0
- .9350	100 N
-1.105	60
-1.275	32
-1.445	22
-1.615	13
-1.785	16
-1.955	8
-2.125	10
-2.295	3
-2.465	5
-2.635	8
X AT TGT2	

Figure 9. Predicted beam spot at the TGT2 location at 500 MeV.

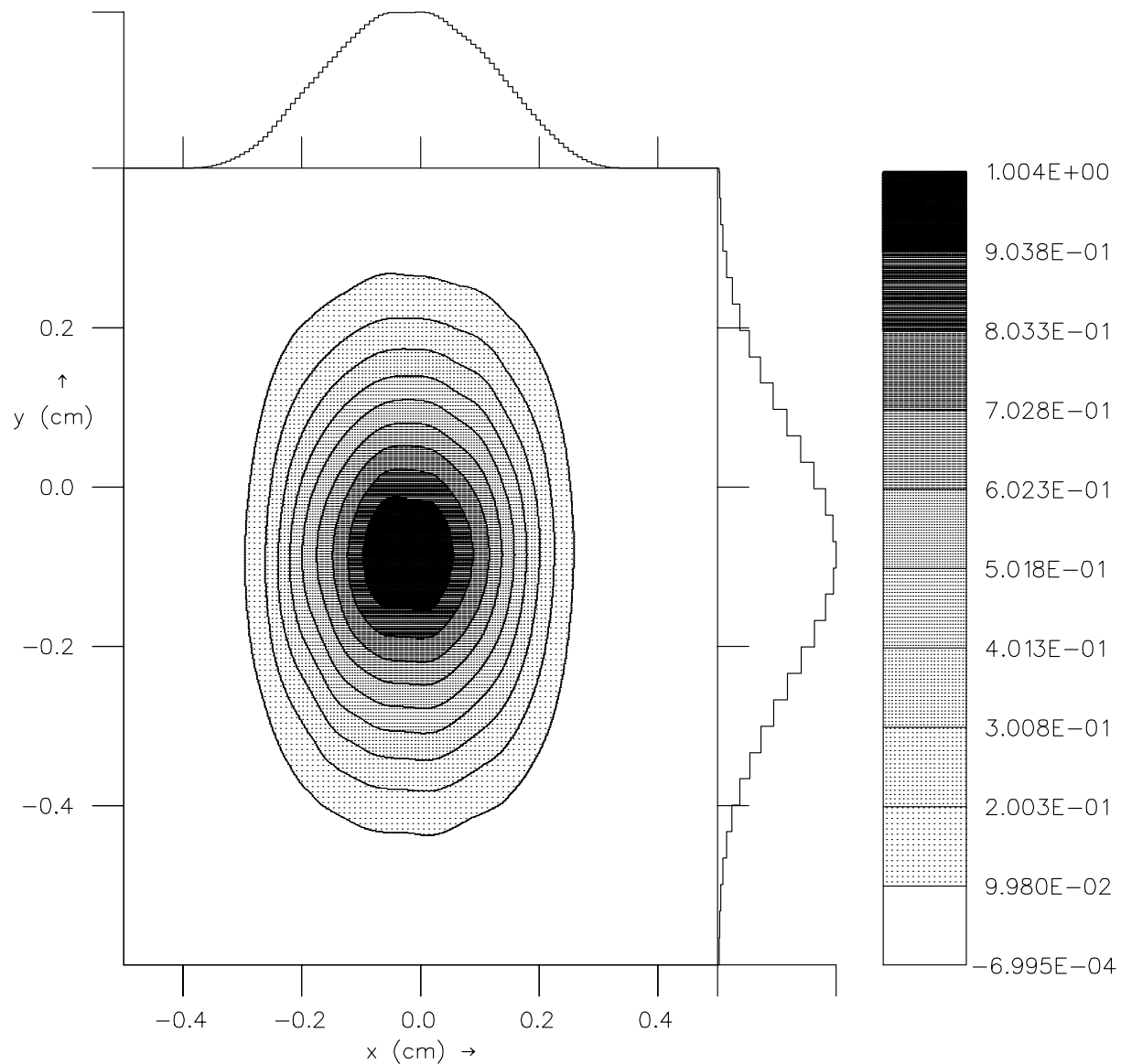


Figure 10. Beam density plot at the TGT2 location at 500 MeV on beam line 2A.

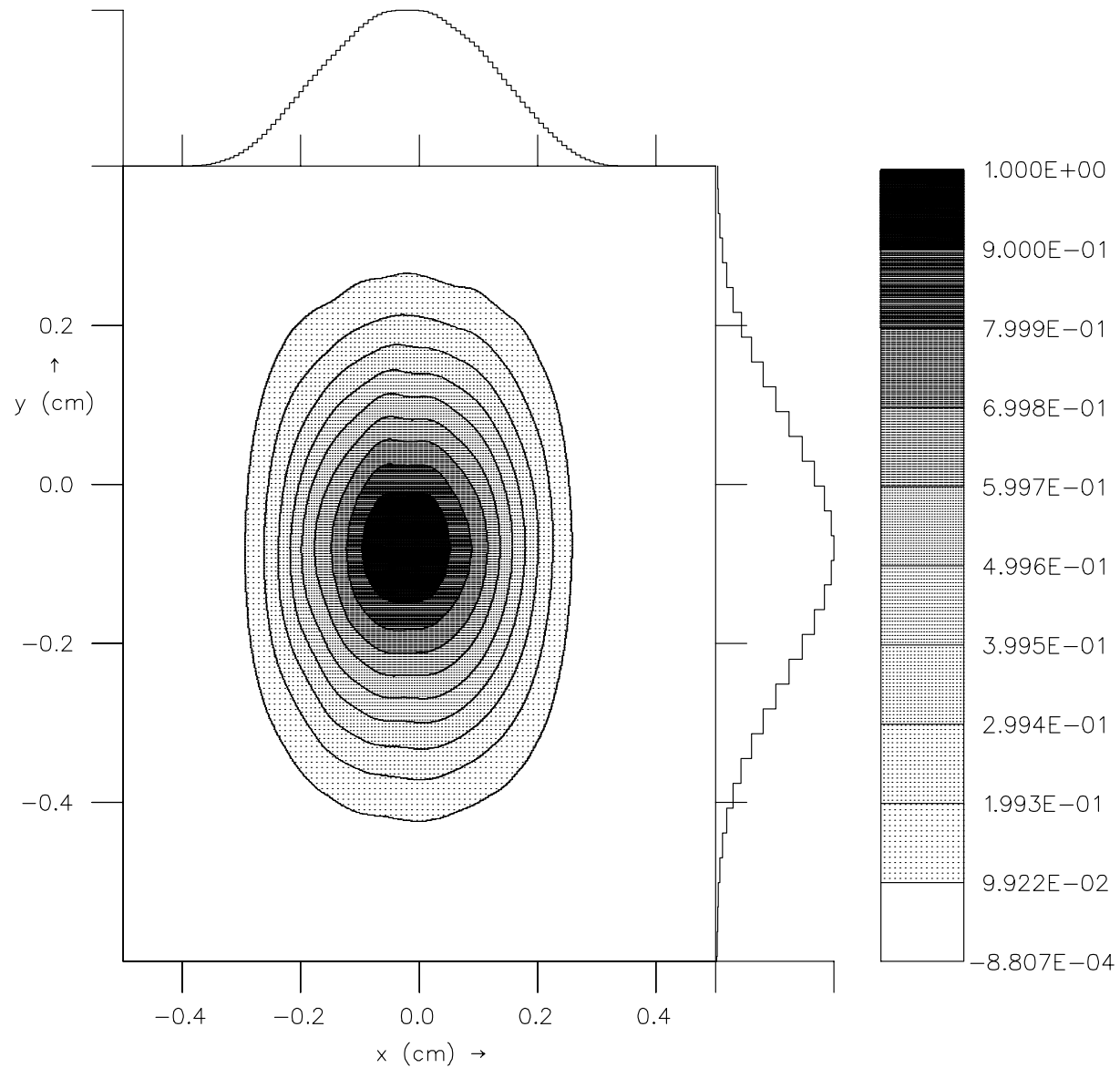


Figure 12. Beam density plot at the TGT2 location at 490 MeV on beam line 2A.

DATA OF 95/10/10 ON 96/06/25 - 480 HEV ON 2-A - NEW TRIPLETS - 2xWst @ WST1 -

Space # 8: Distribution of particles as a function of X AT TGT2 (Element #145) (along HORIZONTAL axis)
& Y at TGT2 (Element #145) (along VERTICAL axis)

Distribution of particles INITIALLY ACCEPTED
COUNTS = 150000.

X PROJECTION

```

           1 1 1 1 1 1
           1 3 6 9 2 5 6 7 6 5 2 9 6 3 1
           2 4 4 4 4 4 7 0 7 5 8 4 8 7 7 6 3 2
           4 2 7 1 7 6 5 3 4 8 7 9 0 1 0 2
  0 0 0 0 0 0 1 7 5 7 1 2 8 7 7 5 2 6 0 7 1 0 1 2 1 0 0 0 0 0 0
+---|-----|-----|-----|-----|-----|-----|-----|+-----+-----+
Y 0.040 |               |               |               |               |               |               |               |
Y 0.8800|               |               |               |               |               |               |               |
0.7200 |               |               |               |               |               |               |               |
0.5600 |               |               |               |               |               |               |               |
A 0.4000 |               |               |               |               |               |               |               |
T 0.2400 |               |               |               |               |               |               |               |
0.8000E-01 |               |               |               |               |               |               |               |
T -0.8000E-01 |               |               |               |               |               |               |               |
G -0.2400 |               |               |               |               |               |               |               |
T -0.4000 |               |               |               |               |               |               |               |
2 -0.5600 |               |               |               |               |               |               |               |
-0.7200 |               |               |               |               |               |               |               |
-0.8800 |               |               |               |               |               |               |               |
-1.040 |               |               |               |               |               |               |               |
+---|-----|-----|-----|-----|-----|-----|-----|-----+-----+
- - - - - - - - - - - - - - - - - - - - - - 0 0 0 0 0 0 0 0 0 0 0 0 0 0 0 0 0 0
+---|-----|-----|-----|-----|-----|-----|-----|-----+-----+
6 5 5 5 4 4 3 3 3 2 2 1 1 0 0 0 0 1 1 1 2 2 3 3 3 4 4 5 5 5
2 8 4 0 6 2 8 4 0 6 2 8 4 0 6 2 2 6 0 4 8 2 6 0 4 8 2 6 0 4 8
X AT TGT2

```

REAL! Distribution of FINAL RUN FOUND HERE
COUNTS = 149986.

X PROJECTION

```

           1 1 1 1 1 1
           1 3 6 9 2 5 6 7 6 5 2 9 6 3 1
           4 5 5 4 5 4 0 6 2 7 3 7 8 7 7 4 3
           1 4 2 5 9 4 8 2 7 0 0 5 0 3 7 1 3 6 7 4 1
  0 2 1 4 0 6 1 2 1 4 3 5 0 0 5 4 8 2 3 1 6 9 8 7 4 2 3 2 2 0 1
+---|-----|-----|-----|-----|-----|-----|-----|-----|-----|+-----+
2.320 |               |               |               |               |               |               |               |               |
2.160 |               |               |               |               |               |               |               |               |
2.000 |               |               |               |               |               |               |               |               |
1.840 |               |               |               |               |               |               |               |               |
1.680 |               |               |               |               |               |               |               |               |
1.520 |               |               |               |               |               |               |               |               |
1.360 |               |               |               |               |               |               |               |               |
1.200 |               |               |               |               |               |               |               |               |
1.040 |               |               |               |               |               |               |               |               |
Y 0.8800 |               |               |               |               |               |               |               |               |
0.7200 |               |               |               |               |               |               |               |               |
0.5600 |               |               |               |               |               |               |               |               |
A 0.4000 |               |               |               |               |               |               |               |               |
T 0.2400 |               |               |               |               |               |               |               |               |
0.8000E-01 |               |               |               |               |               |               |               |               |
T -0.8000E-01 |               |               |               |               |               |               |               |               |
G -0.2400 |               |               |               |               |               |               |               |               |
T -0.4000 |               |               |               |               |               |               |               |               |
2 -0.5600 |               |               |               |               |               |               |               |               |
-0.7200 |               |               |               |               |               |               |               |               |
-0.8800 |               |               |               |               |               |               |               |               |
-1.040 |               |               |               |               |               |               |               |               |
-1.360 |               |               |               |               |               |               |               |               |
-1.520 |               |               |               |               |               |               |               |               |
-1.680 |               |               |               |               |               |               |               |               |
-1.840 |               |               |               |               |               |               |               |               |
-2.000 |               |               |               |               |               |               |               |               |
-2.160 |               |               |               |               |               |               |               |               |
-2.320 |               |               |               |               |               |               |               |               |
-2.480 |               |               |               |               |               |               |               |               |
+---|-----|-----|-----|-----|-----|-----|-----|-----|-----+-----+
- - - - - - - - - - - - - - - - - - - - - - 0 0 0 0 0 0 0 0 0 0 0 0 0 0 0 0 0 0
+---|-----|-----|-----|-----|-----|-----|-----|-----+-----+
6 5 5 5 4 4 3 3 3 2 2 1 1 0 0 0 0 1 1 1 2 2 3 3 3 4 4 5 5 5
2 8 4 0 6 2 8 4 0 6 2 8 4 0 6 2 2 6 0 4 8 2 6 0 4 8 2 6 0 4 8
X AT TGT2

```

Figure 13. Predicted beam spot at the TGT2 location at 480 MeV.

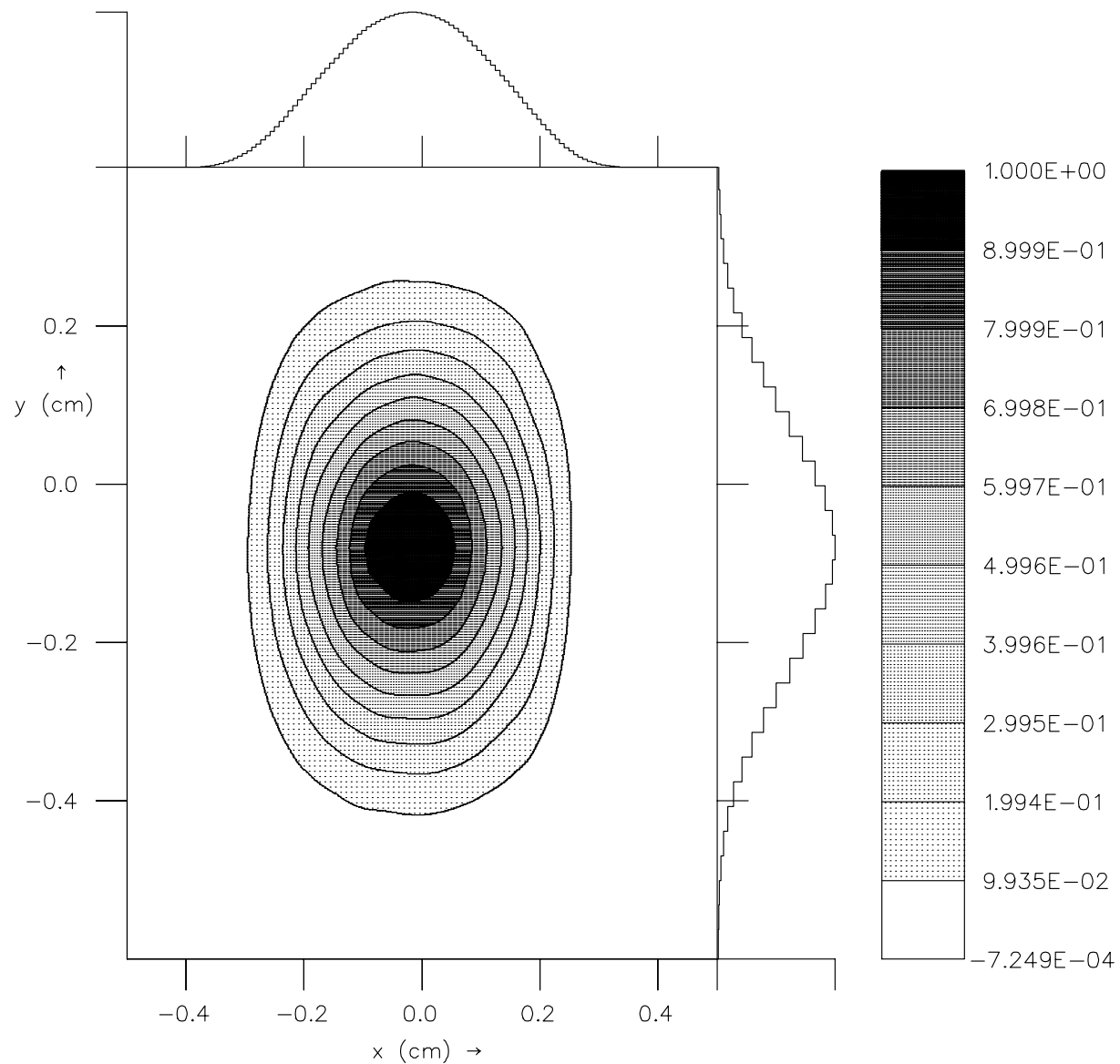


Figure 14. Beam density plot at the TGT2 location at 480 MeV on beam line 2A.

